Defence Technology 17 (2021) 177–184

Contents lists available at ScienceDirect

Defence Technology

journal homepage: www.keaipublishing.com/en/journals/defence-technology

Effect of functionally-graded interphase on the elasto-plastic behavior of nylon-6/clay nanocomposites; a numerical study

Maziyar Bazmara [a], Mohammad Silani [c, *], Iman Dayyani [b]

[a] Department of Mechanical Engineering, University of Houston, TX 77204, United States
[b] Centre for Structures, Assembly and Intelligent Automation, Cranfield University, Cranfield, Bedford MK43 0AL, United Kingdom
[c] Department of Mechanical Engineering, Isfahan University of Technology, Isfahan, 84156-83111, Iran

ARTICLE INFO

Article history:
Received 28 December 2019
Received in revised form
25 January 2020
Accepted 4 March 2020
Available online 8 March 2020

Keywords:
Nylon 6/clay nanocomposites
FG Interphase
Computational homogenization

ABSTRACT

In nanocomposites, the interphase thickness may be comparable to the size of nano-particles, and hence, the effect of interphase layers on the mechanical properties of nanocomposites may be substantial. The interphase thickness to the nano-particle size ratio and properties variability across the interphase thickness are the most important affecting parameters on the overall behavior of nanocomposites. In this study, the effect of properties variability across the interphase thickness on the overall elastic and elasto-plastic properties of a polymeric clay nanocomposite (PCN) using a functionally graded (FG) interphase is investigated in detail. The results of the computational homogenization on the mesoscopic level show that Young's modulus variation of the interphase has a significant effect on the overall elastic response of nanocomposites in a higher clay weight ratio (Wt). Moreover, strength variation through the interphase has a notable effect on the elasto-plastic properties of PCNs. Also, the increase or decrease in stiffness of interphase from clay to matrix and vice versa have a similar effect in the overall behavior of nanocomposites.

1. Introduction

Polymers are one of the most widely used materials in the building, aerospace, and transportation industries [1]. Polymer clay nanocomposites (PCNs) have attracted a lot of attention lately and have become a subject of numerous research studies because of their mechanical properties. As a result of the use of high aspect ratio reinforcement and the extensive surface contact between clays and matrix, these materials have great thermomechanical properties such as low permeability and high heat resistance [2,3]. In the case of thermodynamically equilibrium between homogeneous phases, the surface boundary between different phases is called interface [4]. This very thin area connects the solid surfaces and helps to transfer the load between different phases. Far from the interface, the properties of the matrix are the same as the bulk polymer. However, close to the interface, the properties of the polymer are different from the bulk polymer, as depicted in Fig. 1. This surrounding zone is called interphase. Both Interphase and interface have a significant impact on the thermomechanical properties of nanocomposites [5–9]. The nanometric thickness of interphase leads to limited, expensive, and sometimes impossible experimental measurements.

To overcome the challenges of experimental studies, Molecular Dynamics (MD) method can be used to predict the mechanical properties of the interface layer and interphase zone [10]. For example, Chen et al. [11] used the traction-separation curve of the interphase layer to calculate the peak strength, fracture energy, and splitting distance of the interphase zone. They concluded that the alkyl chain length of surfactants is the key parameter to control the interfacial strength. Kim et al. [12] started from the MD simulations and proposed a multiscale framework to investigate the interphase characteristics of crosslinked epoxy nanocomposites. They showed that crosslinking reduces the interfacial adhesion. The MD results then upscaled to a micromechanical model, and Young's modulus of epoxy nanocomposites as a function of crosslinking was calculated. Odegard et al. [13] employed the molecular structures of

* Corresponding author. Department of Mechanical Engineering, Isfahan University of Technology, Isfahan 84156-83111, Iran.
E-mail addresses: Mbazmara@uh.edu (M. Bazmara), Silani@iut.ac.ir (M. Silani), I.Dayyani@cranfield.ac.uk (I. Dayyani).
Peer review under responsibility of China Ordnance Society

https://doi.org/10.1016/j.dt.2020.03.003

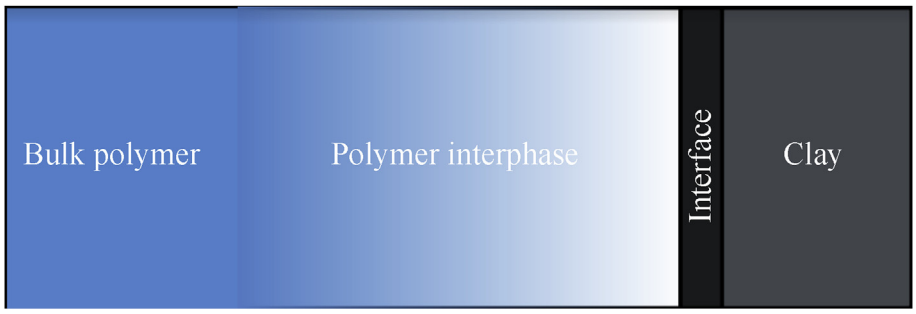

Fig. 1. The schematic illustration of the interface layer and interphase zone in PCNs [9].

three phases nanocomposite using a molecular modeling method that uses coarse-graining and reverse-mapping techniques. They also compared their results with Mori-Tanaka for the elastic properties of a three phases nanocomposite. Fankhänel et al. [14] used the MD method to characterize the elastic properties of interphase layers in boehmite epoxy nanocomposites. They used the atomic strain concept in their study, which allows capturing stiffness gradient at the interphase region. Generally, molecular dynamic simulations are widely used to investigate the adhesion properties of different composites [10].

Although the MD approach reveals many details about the interphase zone, however, it is limited by the size of the representative volume element (RVE) in MD simulations. In order to surmount this challenge, researchers have recommended the use of the finite element method in mesoscale [15–20]. For example, Needleman et al. [21] used the finite element technique to investigate the effect of polymer/carbon nanotube interfacial strength and interphase thickness on the nanocomposite stiffness and strength. They modeled the interfacial behavior by a cohesive relation. Montazeri and Naghdabadi [22] used a multiscale modeling approach to investigate Young's modulus of carbon nanotube (CNT) polymeric nanocomposites. They concluded that it is necessary to consider the interphase zone, and it can't be ignored during the simulations. Almasi et al. [9] proposed a stochastic multiscale framework to analyze the effect of interphase thickness and stiffness on Young's modulus of the PCNs. Their results showed that having a weak interphase zone reduces Young's modulus of clay/epoxy nanocomposites, which is more significant in higher clay contents. Msekh et al. [23] utilized the phase-field technique to study the effect of the interphase properties (thickness, Young's modulus, and strain energy release rate) on the overall tensile strength and fracture properties of the nanocomposite. Hamida and Rabczuk [24], using the framework of the Extended Finite Element Method (XFEM), determined the most affecting parameters on fracture toughness of polymer-based nanocomposites. They concluded that the maximum allowable principal stress and Young's modulus of epoxy are the key parameters.

Besides numerical investigations, several analytical models have been suggested to compute the mechanical properties of nanocomposites in the presence of the interphase region [25]. Pahlavanpour et al. [26] employed analytical homogenization to examine the stiffness of PCNs. They reported that the Mori–Tanaka [27,28] model is the most dependable model to predict Young's modulus of PCNs. The drawback of analytical studies is that they are mainly limited to elastic cases.

In this study, the effects of strength variation through the interphase on the mechanical behavior of PCNs, including elastic modulus, yield strength, and hardening parameters are investigated. A hierarchical multiscale framework is proposed to deal with different length scales. Fig. 2 shows the proposed multiscale framework schematically. A representative volume element (RVE) composed of clays, interphase, and Nylon 6 was created to study the overall stress-strain response of the PCNs. Functionally Graded Interphase (FGI) model is used to examine the effects of strength variation through the interphase on the stress-strain response of PCNs. The results of this study investigate the effects of strength variation through the interphase thickness on the nanocomposite stress-strain curve. Additionally, the effect of weak, soft, and stiff interphases on the overall behavior of nanocomposites is studied.

This paper is organized as follows: in section 2, we describe the detail micromechanical approach to calculate the mechanical properties of PCNs. In section 3, we present the results as well as the effect of important parameters. Finally, section 4 concludes the research manuscript.

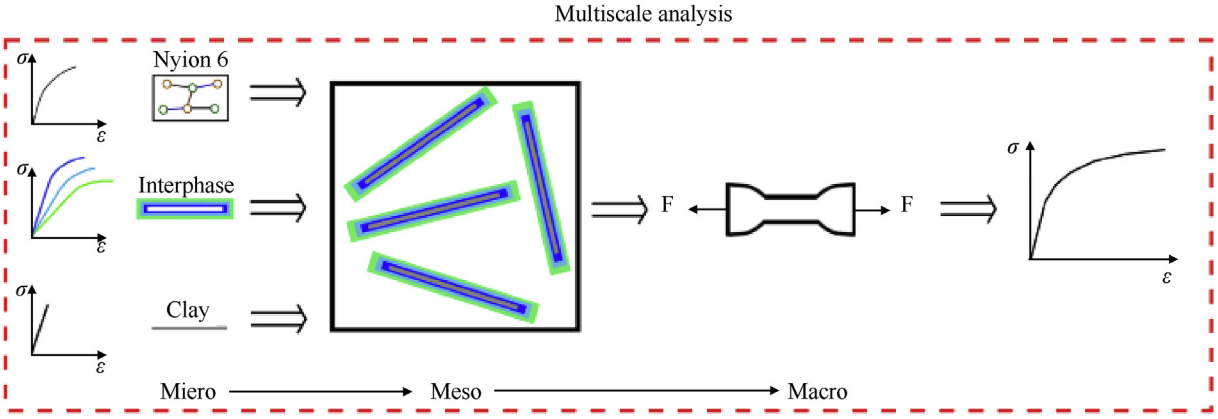

Fig. 2. Schematic flowchart of the proposed multiscale framework.

2. Micromechanical analysis

Multiscale methods use different ways to transfer information between different scales. Hierarchical multiscale methods use a one-way information passing scheme from fine-scale to the coarse-scale. From the computational point of view, hierarchical methods are very efficient for intact materials (in the absence of crack and discontinuity). In contrast to hierarchical methods, semi-concurrent methods use two-way information passing between the fine-scale and the coarse-scale. These methods are very flexible and can easily couple different packages in different scales (e.g., MD packages to the FE software). They can also easily and straightforwardly parallelized, but it is still not very clear how decreasing stress due to material instability at the fine-scale should be reflected in the coarse-scale model. Direct coupling between fine-scale and coarse-scale can be used to overcome instability transfer between different scales. Concurrent multiscale methods use this direct coupling technique and are more suitable for modeling cracks and discontinuities [29].

In this study, employing the finite element method, the elasto-plastic properties of nanocomposites are predicted in the presence of the FG interphase layers. Here, the results are passed from the finer scale to the coarser scale only. Therefore, the hierarchical multiscale method is used. The finite element method is utilized as the approximation method and computational homogenization as the upscaling technique.

2.1. Material behavior and finite element modeling of PCN

A 2D Representative Volume Element (RVE) is created, which consists of clays, FG interphase, and the Nylon 6 matrix. The clays' distribution in the RVE is completely random in terms of their angle and position. The RVE was discretized with plane-stress elements of approximately 2 nm size. Fig. 3 shows the mesh inside RVE and inside the interphase zone. The interphase region is divided into five layers, and each layer has a single element through the thickness that leads to elements with an aspect ratio of 5 in this region.

Experimental results revealed that the thickness of clay platelets is roughly about 1 nm, and their aspect ratio is between 100 and 1000 nm [30–32]. Because clay platelets are much stiffer than Nylon 6, they are considered as linear elastic materials with 221.5 GPa Young's modulus and 0.25 Poisson's ratio [33,34]. In this study, the thickness and the aspect ratio of the platelets are 1 and 100 nm, respectively. Also, clays are distributed fully exfoliated with random orientations. Nylon 6 is a type of polyamide and has elastic-plastic behavior with Elastic modulus of 1.5 GPa and Poisson's ratio of 0.42, in the quasi-static analysis [31]. Additionally, J_2 Plasticity model is used to mimic the plastic behavior of Nylon 6 [30]. This model is described below:

$$\sigma_{eq} = \sigma_Y + R_\infty[1 - \exp(-mp)] \tag{1}$$

In this equation σ_{eq}, σ_Y, R_∞, m and p are Cauchy stress, initial yield stress, hardening modulus, hardening exponent, and accumulated plastic strain, respectively. Table 1 shows the value of each parameter.

The interphase layer entirely encompasses the nanoparticles. It is difficult to measure the precise thickness of the interphase layer. The ratio of the thickness of the interphase layer to the organically modified montmorillonite clay thickness for some polymers such as polyamide 6, polypropylene, and polyamide 12 is in the range of 1 and 4.5 [35]. The thickness of the interphase layer was measured by Zaïri et al. [36] to be approximately 2–3 nm. Xu et al. [37], by MD simulations, determined the interphase thickness of 3 nm. Zolfaghri et al. [38] showed that interphase stiffness is the most influential parameter on the PCNs properties, while thickness has a negligible effect. For this reason, this study is not focused on the effect of different interphase thicknesses, and hence, the interphase thickness was considered as 2 nm.

Msekh et al. [23] reported that there is a bound for interphase Young's modulus in polymer/clay nanocomposites. They considered three cases of weak, soft, and stiff interphases. They used Young's modulus of 1 GPa, 2.75 GPa, and 7.45 GPa for weak, soft, and stiff interphases, respectively. Therefore, the interphase Young's modulus bounded between 1 GPa and 7.45 GPa. In this study, the effect of variation in interphase properties on the mechanical properties of PCNs is investigated, and hence, different distribution functions for strength variation through the interphase region are considered. Four cases of constant, linear, exponential, and polynomial distributions are considered. All Young's modulus distribution functions inside interphase are expressed as below:

$$\text{Constant} \rightarrow \begin{cases} E_{IP} = E_{weak} \\ E_{IP} = E_{soft} \\ E_{IP} = E_{stiff} \end{cases}$$

$$\text{Linear} \rightarrow E_{IP} = E_{weak} + \frac{x-1}{N-1}\left(E_{stiff} - E_{weak}\right) \tag{2}$$

$$\text{Exponential} \rightarrow E_{IP} = E_{weak} e^{d(x-1)}$$

Table 1
Plastic constants of the exponential hardening law for Nylon 6 [30].

Yield Strength /MPa	Hardening Modulus /GPa	Hardening Exponent
14.5	0.034	14.29

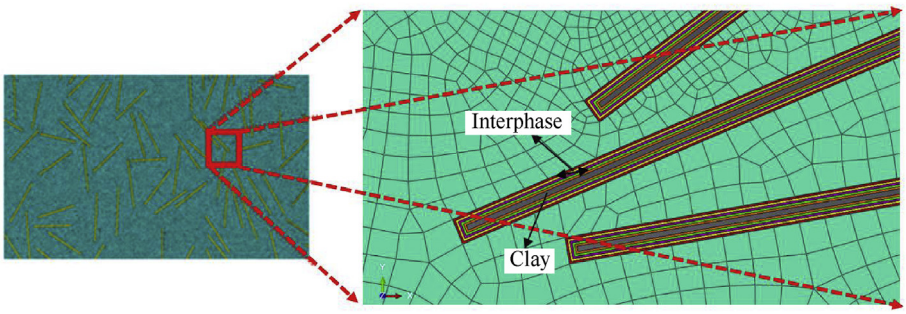

Fig. 3. Two-dimensional representation of the polymer nanocomposites with five interphase layer zone.

$$\text{Polynomial} \rightarrow E_{IP} = E_{weak} + \left(\frac{h+2z}{2h}\right)^{n} \times \left(E_{stiff} - E_{weak}\right)$$

E_{weak}, E_{soft}, and E_{stiff} are 1 GPa, 2.75 GPa, and 7.45 GPa, respectively, as reported by Msekh et al. [28]. E_{IP} is interphase Young's modulus, N is the number of interphase layers (it is five in this study), x is natural numbers from 1 to N, n is polynomial exponent, h is half of the interphase thickness and $z = h\left(\frac{x-1}{N-1} - \frac{1}{2}\right)$ and $d = \frac{1}{N-1}\ln\left(\frac{E_{stiff}}{E_{weak}}\right)$. Each interphase layer behaves as an elasto-plastic material with a scaled stress-strain curve from Nylon 6. This Scale Factor (SF) is the ratio of Young's modulus of each layer to Young's modulus of Nylon 6.

$$SF = \frac{E_i}{E_m} \tag{3}$$

Where E_i and E_m are Young's modulus of interphase layer number i and Young's modulus of the matrix (Nylon 6). Table 2 shows all the material properties used in this article.

2.2. Representative volume element generation

Fig. 4 shows the algorithm which was used to generate the RVE. First, parameters, including clay weight ratio (Wt), size of the RVE, particle dimensions, and mesh size, were calculated. Then, a random sequential addition algorithm (RSA), was used to distribute the nanoclays in the matrix. The intersection between the new particles and all the previous ones was prevented by checking each new particle before creation. If the new particle intersected with one of the existing particles, it was deleted, and another one was created, otherwise, added to the RVE. The code assesses the sufficient number of nanoparticles, which leads to a desirable weight ratio. When the weight ratio of nanoparticles meets the required value, the RVE was meshed. Otherwise, the new particles should be added to the RVE until the desired weight ratio is satisfied. To simplify this algorithm, nanoclays and interphase layers were created simultaneously. At this stage, Young's modulus of each interphase layer must be assigned.

Zolfaghari et al. [38] have shown that the minimum acceptable size of RVE with 1% convergence tolerance is about 500×500 nm^2 in which the randomness doesn't affect the final results. In our study, the size of RVE is chosen to be 1500×1500 nm^2.

2.3. Boundary condition and homogenization algorithm

For a finite-size RVE, three types of Boundary Conditions (BCs) are widely used. These include the Uniform Traction boundary condition (UT), Linear Displacement boundary condition (LD), and mixed boundary condition [39]. Mixed type boundary conditions include periodic boundary conditions [40]. The order relationship of homogenized results motivated us to use PR boundary conditions with the uniaxial strain loading [41].

Volume averaged stresses and strains throughout RVE can be derived by:

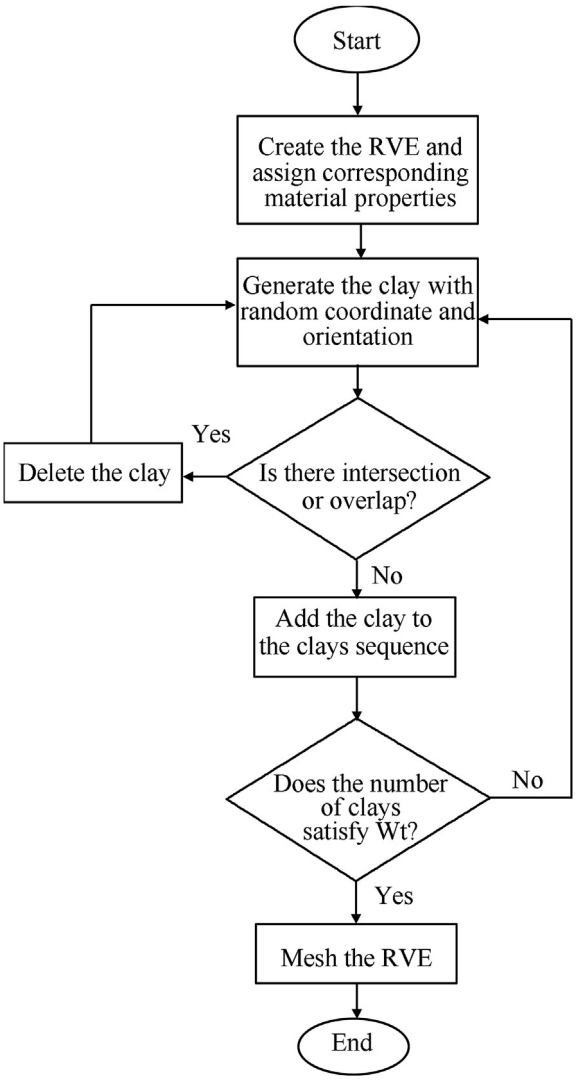

Fig. 4. Python script flow-chart for the PCN including interphase zone generation.

$$\sigma = \frac{1}{\Omega_m}\int_{\Omega_m} \sigma_m d\Omega \tag{4}$$

$$\varepsilon = \frac{1}{\Omega_m}\int_{\Omega_m} \varepsilon_m d\Omega \tag{5}$$

Where σ and ε are average (macroscopic) stress and strain, σ_m and ε_m are the local (microscopic) stress and strain vectors and Ω_m is the volume of the microscopic sample. The stress-strain curve of the material can be upscaled using these homogenized values.

Table 2
Elastic properties of epoxy, clay and interphase zone [23,30]

	Nylon 6	Clay	Weak interphase	Soft interphase	Stiff interphase
E /GPa	1.5	221.5	1	2.75	7.45
Poisson's ratio (υ)	0.42	0.25	0.35	0.35	0.35

3. Results and discussion

3.1. Effects of clay weight ratio and the strength variation through the interphase

RVEs of nanocomposites with four different weight ratios (1%, 2%, 3% and 3.5%) were created. To study the effect of weight ratio, the strength through the interphase was kept constant. The Young's modulus of interphase was set to 7.45 GPa, and the plastic behavior of the interphase was scaled from the Nylon 6 with a scale factor of 7.45/1.5 = 4.97. As shown in Fig. 5, PCN's stiffness increased with an increase in the weight ratio. This is in consonance with the rule of mixtures [42,43].

To evaluate the effect of interphase on the elasto-plastic properties of PCNs, the following power-law curve was fitted to the curves of Fig. 5

$$\sigma = C\varepsilon^n \tag{6}$$

where C is the hardening coefficient, and n is the strain hardening exponent. The strain hardening exponent usually lies between zero and 0.5. The higher value of n shows the more pronounced strain hardening character of the material.

After curve fitting, the parameters of the fitted curve are shown in Table 3 which displays that the hardening coefficient (C) of PCNs increased noticeably (as high as 40%) as the weight ratio increased and the strain hardening exponent (n) decreased by 5.8%, 9%, 15.3%, and 16.4% in for weight ratio of 1%, 2%, 3%, and 3.5% respectively, compared to pure Nylon 6. This is in agreement with the results published by Yang et al. [44] in which the secant moduli method was adopted to investigate the effects of interfacial defects on the mechanical properties of nanocomposites via MD simulations and continuum micromechanics. They concluded that the slope of the stress-strain curve increases as the corresponding interfacial compliance increases.

To analyze the effects of strength variation through the interphase, RVEs with different distribution functions were created. The weight ratio of the particles was kept constant for all cases as; a) Wt = 1%, b) Wt = 2%, c) Wt = 3%, d) Wt = 3.5%. As shown in Figs. 6–9, the results illustrated that the nanocomposite's Young's modulus increased with an increase in interphase Young's modulus. This is in agreement with the results obtained by Zolfaghari et al. [38]. They compared Young's modulus of three-phase random composites with different interphase stiffness and thickness using finite element and stochastic methods. They reported

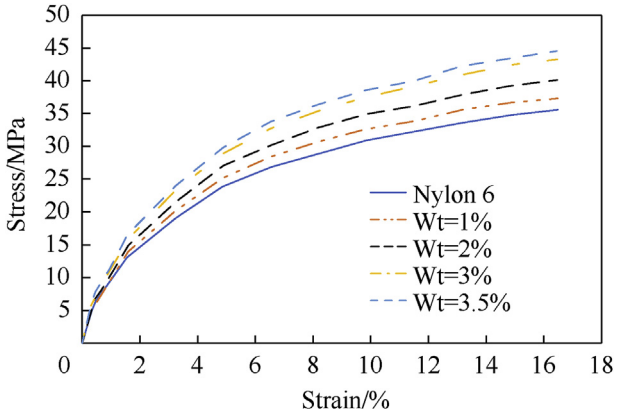

Fig. 5. Averaged stress-strain curves for RVEs with random distribution and orientation of clays; particle weight ratios Wt = 1%, 2%, 3%, and 3.5%. E_{IP} = 7.45 GPa for all cases.

Table 3
Hardening parameters of polymer/clay nanocomposites for different weight ratios.

Hardening parameters	Wt = 0%	Wt = 1%	Wt = 2%	Wt = 3%	Wt = 3.5%
C /MPa	13.05	15.76	16.75	17.95	18.38
n	0.3617	0.3405	0.3291	0.3065	0.3025

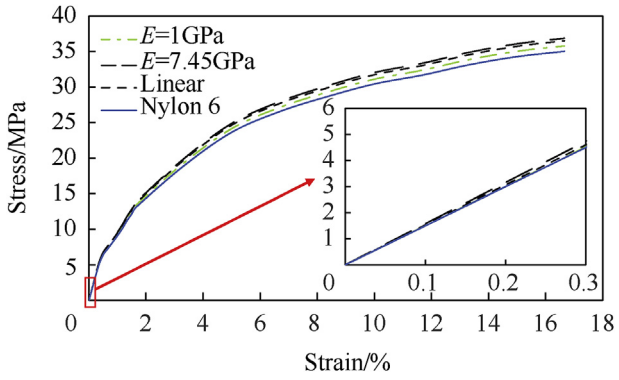

Fig. 6. Average stress–strain curves for representative volume elements with random distribution and orientation of clays (1% weight ratio).

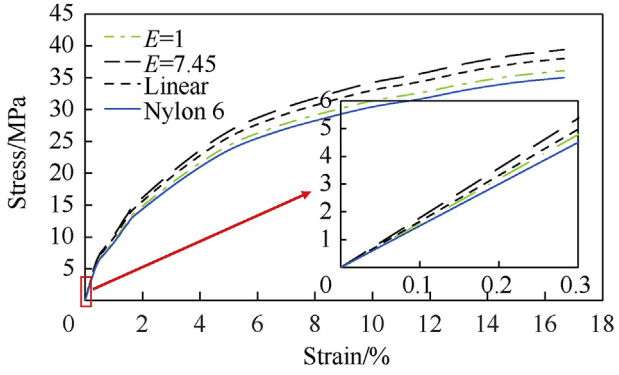

Fig. 7. Average stress-strain curves for representative volume elements with random distribution and orientation of clays (2% weight ratio).

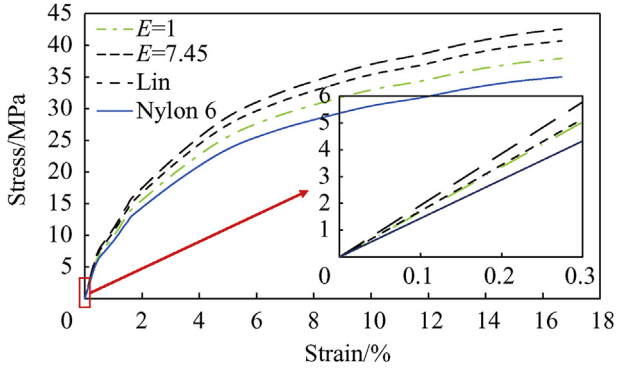

Fig. 8. Average stress-strain curves for representative volume elements with random distribution and orientation of clays (3% weight ratio).

that Young's modulus of nanocomposites expanded by increasing the interphase stiffness. In all cases, interphase stiffness decreased from clay to matrix. Due to the same trend for different interphase's properties, only the results of three different Young's modulus

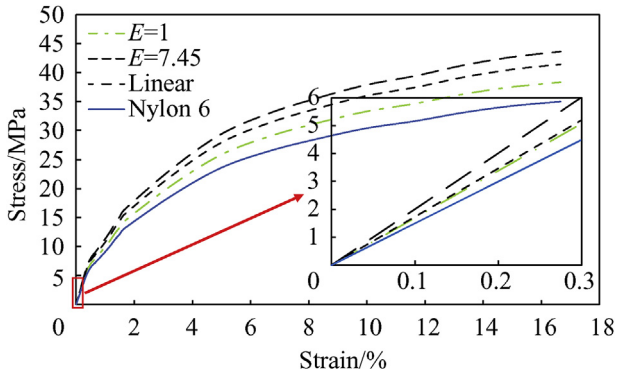

Fig. 9. Average stress-strain curves for representative volume elements with random distribution and orientation of clays (3.5% weight ratio).

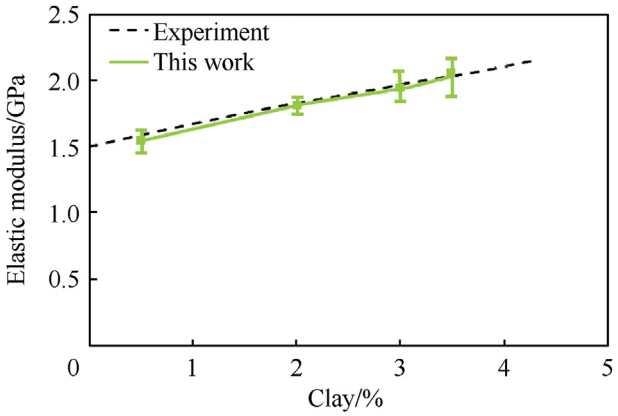

Fig. 10. Comparing Young's modulus for numerical and experimental [31] for different weight ratios.

variation of the interphase (constant with $E_{IP} = 7.45$ GPa, constant with $E_{IP} = 1$ GPa, and linear) are shown in the following Figs. 6–9, but Table 4 shows the results for all cases. Table 4 summarizes all the results obtained from Figs. 6–9 for PCNs Young's modulus. Based on the results of Table 4, using different functions to create Young's modulus variation of the interphase can affect Young's modulus of PCNs up to 14% for the case in which weight ratio is 3.5%.

As shown in Fig. 10, the mean value of Young's modulus for different weight ratios is illustrated. The results are extracted from 20 realizations for each weight ratio. For each realization, yield strength is calculated for a 0.2% offset based on homogenized outputs (ASTM D638). Numerical predictions cover experimental results within their standard deviation region. The results of Fig. 10 are in agreement with available experimental results in the literature [31]. It should be noted that in all cases, interphase Young's modulus is kept constant, $E_{IP} = 7.45$ GPa.

Also, to explore the effect of strength variation through the interphase on PCNs' stress-strain curve, hardening constants of PCNs were calculated in Table 5. The results explain that the strength coefficient (C) of PCNs increased, and the strain-hardening exponent (n) decreased as the weight ratio increased. This is in consensus with the results reported by Zare and Garmabi [35]. The authors of that paper worked on the quantification of the mechanical properties of interphase in the polymer clay nanocomposites. Using Ji and Pukanszky micromechanical models, thickness and strength of interphase were measured. They showed that the PCNs became stronger as the clays' weight ratio and interphase thickness increased.

As shown in Fig. 11, the mean value of yield strength for different weight ratios is illustrated. The same process as what was adopted to plot Fig. 7 is used for plotting data in Fig. 11. The results are extracted from 20 realizations for each weight ratio. For each realization, yield strength is calculated for a 0.2% offset based on homogenized outputs (ASTM D638). Numerical predictions cover experimental results within their standard deviation region. The results of Fig. 11 are in consensus with available experimental results published by He et al. [31]. It should be noted that in all cases, interphase Young's modulus is kept constant, $E_{IP} = 7.45$ GPa.

3.2. Effect of increase and decrease of interphase stiffness from clay to matrix

Here, we compared our predicted results for inverse strength variation through the interphase. Moreover, we compared the results of the average amount of interphase stiffness for each distribution. The weight ratio of the particles was kept constant for all cases to Wt = 3.5%. As shown in Table 6, the results displayed that an increase or decrease in interphase stiffness for all distributions had no effect on Young's modulus of PCN. In addition, according to Table 6, it is obvious that Young's modulus of PCN for each distribution was lower than the state in which Young's modulus of all interphase layers was uniformly equal to the average of that distribution.

4. Conclusion

In this study, the effects of strength variation through the interphase on the mechanical behavior of clay/epoxy nanocomposites, including elastic modulus, yield strength, and hardening parameters were investigated, employing the micromechanical analysis and computational homogenization technique. The finite element models of the representative volume elements (RVEs) were created according to a procedure which guaranteed the randomness of the RVEs. Stress-strain curves were computed using a computational homogenization method. The results of this study showed that the effects of the interphase layer on elastic modulus and yield strength of PCNs are more significant at higher weight ratios while an increase or decrease in stiffness of the interphase from clay to the matrix and vice versa have a similar effect on the mechanical behavior of nanocomposites. In that case, Young's modulus of PCN for each distribution was lower than the

Table 4
Young's modulus (GPa) of polymer/clay nanocomposites according to different weight ratio and strength variation through the interphase.

Distribution function → weight ratio↓	$E = 1$ GPa	$E = 2.75$ GPa	$E = 7.45$ GPa	Exp	Linear	polynomial $N = 0.1$
Wt = 1%	1.533	1.564	1.599	1.560	1.564	1.569
Wt = 2%	1.594	1.657	1.788	1.648	1.657	1.667
Wt = 3%	1.675	1.774	1.924	1.709	1.714	1.790
Wt = 3.5%	1.694	1.810	2.009	1.729	1.736	1.824

Table 5
Hardening parameters of PCNs for different strength variations through the interphase.

Clay weight ratio	Hardening parameters	E = 1 GPa	E = 2.75 GPa	E = 7.45 GPa	Exponential	Linear	polynomial N = 0.1
Wt = 1%	C /MPa	15.08	15.35	15.76	15.52	15.58	15.63
	n	0.3601	0.3584	0.3405	0.3421	0.3424	0.3515
Wt = 2%	C /MPa	15.20	15.82	16.75	16.19	16.34	16.46
	n	0.3597	0.3502	0.3291	0.3325	0.3331	0.3389
Wt = 3%	C /MPa	15.34	16.39	17.95	17.02	17.27	17.46
	n	0.3585	0.3415	0.3065	0.3220	0.3169	0.3201
Wt = 3.5%	C /MPa	15.35	16.49	18.38	17.17	17.48	17.68
	n	0.3584	0.3398	0.3025	0.3211	0.3149	0.3195

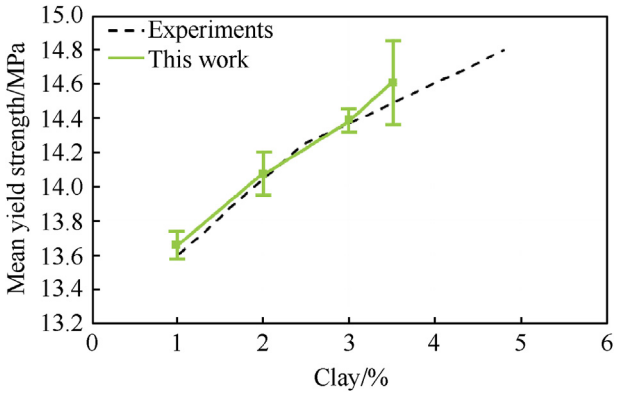

Fig. 11. Comparing the yield strength for numerical and experimental [31] for different weight ratios.

Table 6
Young's modulus (GPa) of polymer/clay nanocomposites according to different weight ratio and strength variation through the interphase for 3.5% weight ratio.

Distribution Function	E_{PCN} /GPa	E_{avg} interphase /GPa
Constant with E = 1	1.694	1
Constant with E = 2.75	1.81	2.75
Constant with E = 7.45	2.01	7.45
Exponential	1.729	3.4676
Inv. Exponential	1.730	
Constant E = 3.4676	1.822	
Linear	1.736	4.225
Inv. Linear	1.736	
Constant E = 4.225	1.835	
Polynomial n = 0.1	1.824	5.87
Inv. Polynomial n = 0.1	1.823	
Constant E = 5.87	1.962	

state in which Young's modulus of all interphase layers equals to the average value of that distribution. This simplification can lead to an error as high as 8% for the prediction of PCNs elastic modulus. The mean values of yield strength and elastic modulus for different weight ratios were calculated by using the extracted results from 20 realizations for each weight ratio. For both mean yield strength and mean elastic modulus, the experimental results are within the standard deviation of the numerical predictions.

Declaration of competing interest

The authors declare that they have no known competing financial interests or personal relationships that could have appeared to influence the work reported in this paper.

Acknowledgements

The authors thank the financial support of the Iran National Science Foundation (INSF).

References

[1] Ho MW, Lam CK, Lau KT, Ng DH, Hui D. Mechanical properties of epoxy-based composites using nanoclays. Compos Struct 2006;75(1–4):415–21.
[2] Couch EL, Grim RE. Boron fixation by illites. Clay Clay Miner 1968;16(3):249–56.
[3] Jordan J, Jacob KI, Tannenbaum R, Sharaf MA, Jasiuk I. Experimental trends in polymer nanocomposites—a review. Mater Sci Eng A 2005;393(1–2):1–11.
[4] Adamson AW, Gast AP. Physical chemistry of surfaces, vol. 150. New York: Interscience publishers; 1967. p. 180.
[5] Safaei M, Sheidaei A, Baniassadi M, Ahzi S, Mashhadi MM, Pourboghrat F. An interfacial debonding-induced damage model for graphite nanoplatelet polymer composites. Comput Mater Sci 2015;96:191–9.
[6] Ohji T, Hirano T, Nakahira A, Niihara K. Particle/matrix interface and its role in creep inhibition in alumina/silicon carbide nanocomposites. J Am Ceram Soc 1996;79(1):33–45.
[7] Pukánszky B. Interfaces and interphases in multicomponent materials: past, present, future. Eur Polym J 2005;41(4):645–62.
[8] Roy M, Nelson JK, MacCrone RK, Schadler LS, Reed CW, Keefe R. Polymer nanocomposite dielectrics-the role of the interface. IEEE Trans Dielectr Electr Insul 2005;12(4):629–43.
[9] Almasi A, Silani M, Talebi H, Rabczuk T. Stochastic analysis of the interphase effects on the mechanical properties of clay/epoxy nanocomposites. Compos Struct 2015;133:1302–12.
[10] Zhou S, Vu-Bac N, Arash B, Zhu H, Zhuang X. Interface characterization between polyethylene/silica in engineered cementitious composites by molecular dynamics simulation. Molecules 2019;24(8):1497.
[11] Chen Y, Chia JYH, Su ZC, Tay TE, Tan VBC. Mechanical characterization of interfaces in epoxy-clay nanocomposites by molecular simulations. Polymer 2013;54(2):766–73.
[12] Kim B, Choi J, Yang S, Yu S, Cho M. Multiscale modeling of interphase in crosslinked epoxy nanocomposites. Compos Part B Eng 2017;120:128–42.
[13] Odegard GM, Clancy TC, Gates TS. Modeling of the mechanical properties of nanoparticle/polymer composites. In: Characterization of nanocomposites. Jenny Stanford Publishing; 2017. p. 319–42.
[14] Fankhänel J, Arash B, Rolfes R. Elastic interphase properties of nanoparticle/epoxy nanocomposites: a molecular dynamics study. Compos Part B Eng 2019;176:107211.
[15] Ayatollahi MR, Shadlou S, Shokrieh MM. Multiscale modeling for mechanical properties of carbon nanotube reinforced nanocomposites subjected to different types of loading. Compos Struct 2011;93(9):2250–9.
[16] Spanos PD, Kontsos A. A multiscale Monte Carlo finite element method for determining mechanical properties of polymer nanocomposites. Probabilist Eng Mech 2008;23(4):456–70.
[17] Tserpes KI, Papanikos P, Labeas G, Pantelakis SG. Multi-scale modeling of tensile behavior of carbon nanotube-reinforced composites. Theor Appl Fract Mech 2008;49(1):51–60.
[18] Tserpes KI, Labeas G, Pantelakis S. Multi-scale modeling of the mechanical response of plain weave composites and cellular solids. Theor Appl Fract Mech 2010;54(3):172–9.
[19] Shokrieh MM, Rafiee R. Stochastic multi-scale modeling of CNT/polymer composites. Comput Mater Sci 2010;50(2):437–46.
[20] Hamdia KM, Silani M, Zhuang X, He P, Rabczuk T. Stochastic analysis of the fracture toughness of polymeric nanoparticle composites using polynomial chaos expansions. Int J Fract 2017;206(2):215–27.
[21] Needleman A, Borders TL, Brinson LC, Flores VM, Schadler LS. Effect of an interphase region on debonding of a CNT reinforced polymer composite. Compos Sci Technol 2010;70(15):2207–15.
[22] Montazeri A, Naghdabadi R. Investigation of the interphase effects on the mechanical behavior of carbon nanotube polymer composites by multiscale modeling. J Appl Polym Sci 2010;117(1):361–7.
[23] Msekh MA, Cuong NH, Zi G, Areias P, Zhuang X, Rabczuk T. Fracture properties prediction of clay/epoxy nanocomposites with interphase zones using a phase field model. Eng Fract Mech 2018;188:287–99.
[24] Hamdia KM, Rabczuk T. July. Key parameters for fracture toughness of particle/polymer nanocomposites; sensitivity analysis via XFEM modeling

approach. In: Fracture, fatigue and wear. Singapore: Springer; 2018. p. 41–51.
[25] Hamdia KM, Zhuang X, He P, Rabczuk T. Fracture toughness of polymeric particle nanocomposites: evaluation of models performance using Bayesian method. Compos Sci Technol 2016;126:122–9.
[26] Pahlavanpour M, Moussaddy H, Ghossein E, Hubert P, Lévesque M. Prediction of elastic properties in polymer–clay nanocomposites: analytical homogenization methods and 3D finite element modeling. Comput Mater Sci 2013;79:206–15.
[27] Mori T, Tanaka K. Average stress in matrix and average elastic energy of materials with misfitting inclusions. Acta Metall 1973;21(5):571–4.
[28] Benveniste Y. A new approach to the application of Mori-Tanaka's theory in composite materials. Mech Mater 1987;6(2):147–57.
[29] Talebi H, Silani M, Bordas SP, Kerfriden P, Rabczuk T. A computational library for multiscale modeling of material failure. Comput Mech 2014;53(5):1047–71.
[30] Song S, Chen Y, Su Z, Quan C, Tan VB. Multiscale modeling of damage progression in nylon 6/clay nanocomposites. Compos Sci Technol 2014;100:189–97.
[31] He C, Liu T, Tjiu WC, Sue HJ, Yee AF. Microdeformation and fracture mechanisms in polyamide-6/organoclay nanocomposites. Macromolecules 2008;41(1):193–202.
[32] Kojima Y, Usuki A, Kawasumi M, Okada A, Fukushima Y, Kurauchi T, Kamigaito O. Mechanical properties of nylon 6-clay hybrid. J Mater Res 1993;8(5):1185–9.
[33] Wang K, Chen L, Wu J, Toh ML, He C, Yee AF. Epoxy nanocomposites with highly exfoliated clay: mechanical properties and fracture mechanisms. Macromolecules 2005;38(3):788–800.
[34] Chen B, Evans JR. Elastic moduli of clay platelets. Scripta Mater 2006;54(9):1581–5.
[35] Zare Y, Garmabi H. Thickness, modulus and strength of interphase in clay/polymer nanocomposites. Appl Clay Sci 2015;105:66–70.
[36] Zaïri F, Gloaguen JM, Naït-Abdelaziz M, Mesbah A, Lefebvre JM. Study of the effect of size and clay structural parameters on the yield and post-yield response of polymer/clay nanocomposites via a multiscale micromechanical modelling. Acta Mater 2011;59(10):3851–63.
[37] Xu W, Zeng Q, Yu A. Young's modulus of effective clay clusters in polymer nanocomposites. Polymer 2012;53(17):3735–40.
[38] Zolfaghari H, Silani M, Yaghoubi V, Jamshidian M, Hamouda AM. Stochastic analysis of interphase effects on elastic modulus and yield strength of nylon 6/clay nanocomposites. Int J Mech Mater Des 2019;15(1):109–23.
[39] Temizer I. Lecture notes micromechanics analysis of heterogeneous materials. Department of Mechanical Engineering Bilkent University; 2007.
[40] Nemat-Nasser S, Hori M. Micromechanics: overall properties of heterogeneous materials. Elsevier; 2013.
[41] Hazanov S, Huet C. Order relationships for boundary conditions effect in heterogeneous bodies smaller than the representative volume. J Mech Phys Solid 1994;42(12):1995–2011.
[42] Alger M. Polymer science dictionary. Springer Science & Business Media; 1996.
[43] Askeland DR, Phulé PP, Wright WJ, Bhattacharya DK. The science and engineering of materials. 2003.
[44] Yang S, Yu S, Ryu J, Cho JM, Kyoung W, Han DS, Cho M. Nonlinear multiscale modeling approach to characterize elastoplastic behavior of CNT/polymer nanocomposites considering the interphase and interfacial imperfection. Int J Plast 2013;41:124–46.

2020-03-08

Effect of functionally-graded interphase on the elasto-plastic behavior of nylon-6/clay nanocomposites; a numerical study

Bazmara, Maziyar

Elsevier

Bazmara M, Silani M, Dayyani I. (2021) Effect of functionally-graded interphase on the elasto-plastic behavior of nylon-6/clay nanocomposites; a numerical study. Defence Technology, Volume 17, Issue 1, February 2021, pp. 177-184

https://doi.org/10.1016/j.dt.2020.03.003